Journal of
MARINE RESEARCH

Volume 37, Number 1

Poleward heat flux and conversion of available potential energy in Drake Passage

by Harry L. Bryden[1]

ABSTRACT

Energetic fluctuations of periods longer than a day are found to transport heat poleward in the Drake Passage. Heat fluxes due to these low-frequency motions are large enough to account for all of the poleward heat transport across the polar front necessary to balance the heat lost to the atmosphere by waters around the Antarctic continent. Because of the poleward density gradient associated with the Antarctic Circumpolar Current in this region, these heat fluxes are associated with a conversion of available potential energy into eddy potential and kinetic energies. The rate of conversion is found to be approximately equal to the rate at which wind puts energy into the water column. Comparison is made with the baroclinic instability model which predicts conversion of available potential energy. The vertical phase function, which is suggested by several authors to be a signature of the instability process, proved difficult to observe in these observations. The signature of the instability process for these observations is that temperature and poleward velocity are nearly in phase. Associated with this signature are a 90° phase difference between poleward and eastward velocity components and a dominance of energy in the counterclockwise half of the rotary spectrum. The relationship between poleward heat flux and large-scale temperature gradient is found to agree within a factor of 2 with that obtained from consideration of the instability process in the atmosphere. Such agreement suggests that heat fluxes due to low-frequency motions may be parameterized in terms of large-scale temperature gradients in models of ocean circulation.

1. Introduction

During the last decade, energetic current fluctuations with periods longer than a day have been found in many regions of the ocean (Swallow, 1971; Koshlyakov

1. Woods Hole Oceanographic Institution, Woods Hole, Massachusetts, 02543, U.S.A.

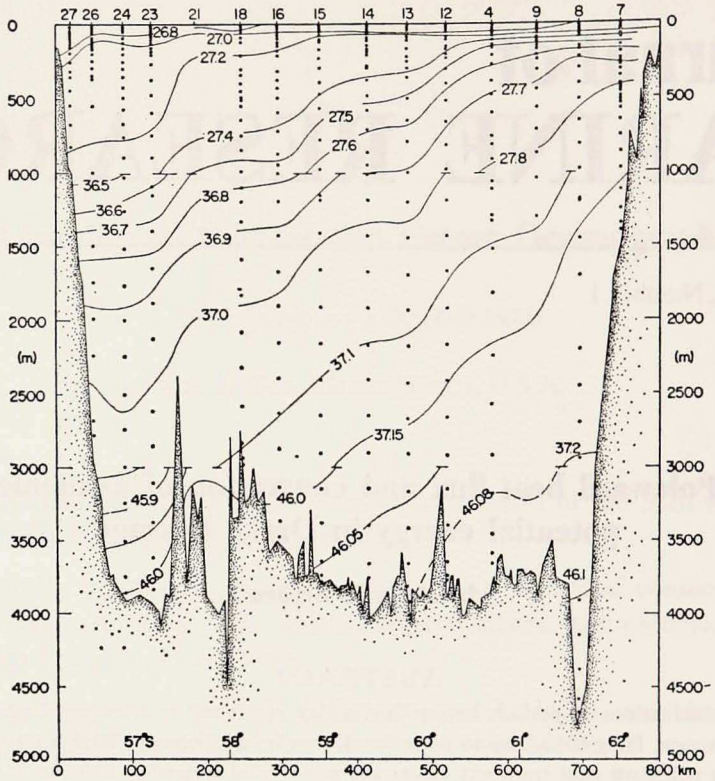

Figure 1. Density distribution in the Drake Passage (Nowlin, Whitworth and Pillsbury, 1977, Figure 4d). The section extends from South America in the north to Antarctica in the south. For depths between 0 and 1000 m, σ_θ is contoured; between 1000 and 3000 m, σ_2 is contoured; below 3000 m, σ_4 is contoured.

and Grachev, 1973; Gould, Schmitz and Wunsch, 1974; Bernstein and White, 1974). The mechanism for generating these fluctuations is not established (Rhines, 1977), although the most prevalent explanation is that they are generated by conversion of available potential energy by the process of baroclinic instability (Gill, Green and Simmons, 1974; Robinson and McWilliams, 1974; Holland and Lin, 1975). And the effect of these fluctuations on the mean circulation of the ocean is as yet unclear although their momentum flux gradients may drive a mean circulation, as suggestion by Schmitz (1977) for the deep circulation in the western North Atlantic, or their heat fluxes may provide the poleward heat flux required of the ocean circulation (Vonder Haar and Oort, 1973).

Because of the presence of a large poleward density gradient, the region of the Antarctic Circumpolar Current provides a favorable environment for studies of the generation of low-frequency current fluctuations and their effects on mean circula-

tion. The large meridional slopes of density surfaces (Fig. 1) provide a reservoir of available potential energy from which fluctuations may draw eddy kinetic and potential energies by the baroclinic instability mechanism (Eady, 1949). Because of the sign of the meridional density gradient, conversion of available potential energy into eddy energies entails a poleward flux of heat, which Gordon (1975) has shown must occur in the region of the Circumpolar Current to balance the heat lost to the atmosphere by waters around the Antarctic continent. In addition, the fluctuations may act to maintain the Circumpolar Current by feeding kinetic energy into the mean current as suggested by Thompson (1971) or they may act as a drag on the Circumpolar Current by transporting eastward momentum away from the mean current.

In this work, current and temperature measurements in the Drake Passage are used to estimate poleward heat fluxes and to investigate the mechanism by which these heat fluxes are effected. An assumption that these heat fluxes are typical of the entire circumpolar region allows the amount of poleward heat flux due to the fluctuations to be compared with the total amount of heat transport across the polar frontal zone estimated by Gordon (1975). Because poleward heat fluxes in this region are associated with conversion of available potential energy into eddy energy, the characteristics of the current and temperature fluctuations are compared with those predicted by the baroclinic instability model. While the proximity of land barriers on the north and south and of an archipelago to the east could make comparisons of Drake Passage measurements with a mid-ocean baroclinic instability model inappropriate, the inherent spatial scales of the fluctuations such as the Rossby radius of deformation,

$$\frac{\int_{-H}^{0} N dz}{f\pi} = 20 \text{ km},$$

and the transition scale between linear and nonlinear dynamics $\sqrt{U/\beta} = 90$ km for $U = 10$ cms^{-1}, are much smaller than the distance across the Passage, 700 km, or the distance to the archipelago, 1000 km. Thus the fluctuations, at least in the center of the Passage, should not be strongly affected by boundaries and comparisons with the instability model should be appropriate.

The array of current and temperature measurements used in this study was deployed from March, 1975, to February, 1976, in a nearly north-south line across the Drake Passage. The long-term array of six moorings was designed to investigate the temporal and spatial variability of the Antarctic Circumpolar Current. Each of the moorings, numbered 2 (northernmost), 4, 8, 10, 12, 14 (southernmost), had a current meter also measuring temperature at approximately 2700 m depth. On mooring 10 in the central part of the Passage, current meters were deployed at 1020 m and 1520 m in addition to the deep current meter at 2520 m depth. Pills-

bury, Whitworth, Nowlin and Sciremammano (1979) have described these measurements and Bryden and Pillsbury (1977) have used the deep current measurements to estimate the variability of the transport of the Antarctic Circumpolar Current through Drake Passage.

2. Heat flux calculations

To estimate heat fluxes due to low-frequency motions, hourly measurements of current and temperature are first put through a low-pass filter with half-power at 0.6 cycles per day (Mooers *et al.*, 1968) to eliminate high-frequency fluctuations. Currents are represented in down-channel (u, 62°T, eastward) and cross-channel (v, 152°T, poleward) components. The down-channel direction is chosen to match the direction of geostrophic current shear determined from hydrographic sections (Nowlin, Whitworth and Pillsbury, 1977) so the cross-channel direction is the direction of the horizontal density and temperature gradients associated with the Antarctic Circumpolar Current. Heat fluxes are then calculated by multiplying values of temperature and velocity for each current meter after removing record-length averaged values:

$$\overline{u'T'} = \overline{(u - \bar{u})\,(T - \bar{T})}$$

$$\overline{v'T'} = \overline{(v - \bar{v})\,(T - \bar{T})}$$

$$\text{Eastward Heat Flux} = 0.98 \text{ cal cm}^{-3}\,{}^{\circ}C^{-1} \times \overline{u'T'}$$

$$\text{Poleward Heat Flux} = 0.98 \text{ cal cm}^{-3}\,{}^{\circ}C^{-1} \times \overline{v'T'}$$

where the bars denote record-length averages and primes denote deviations from record-length averages. Poleward heat fluxes due to low-frequency motions are positive for all current meters except for that on the southernmost mooring 14 (Fig. 2a). Eastward heat fluxes are both positive and negative but generally have magnitudes smaller than the poleward heat fluxes (Fig. 2b). At mooring 10 where measurements were made at three depths, heat fluxes are larger at shallower depths.

From hourly measurements, heat fluxes due to high-frequency motions are also estimated. While such heat fluxes are an order of magnitude smaller than heat fluxes due to low-frequency motions, they may be poorly estimated from these measurements. Because the least bit recorded for temperature corresponded to the change in temperature over approximately 10 m depth associated with the mean stratification, temperature fluctuations due to internal waves with amplitudes less than 10 m are not resolved. If motions with amplitudes less than 10 m contribute significantly to the heat fluxes for high-frequency fluctuations, these heat fluxes are poorly estimated. Thus, it is appropriate to conclude only that heat fluxes due to high-frequency motions of amplitude more than 10 m in the vertical are small compared with heat fluxes due to low-frequency motions.

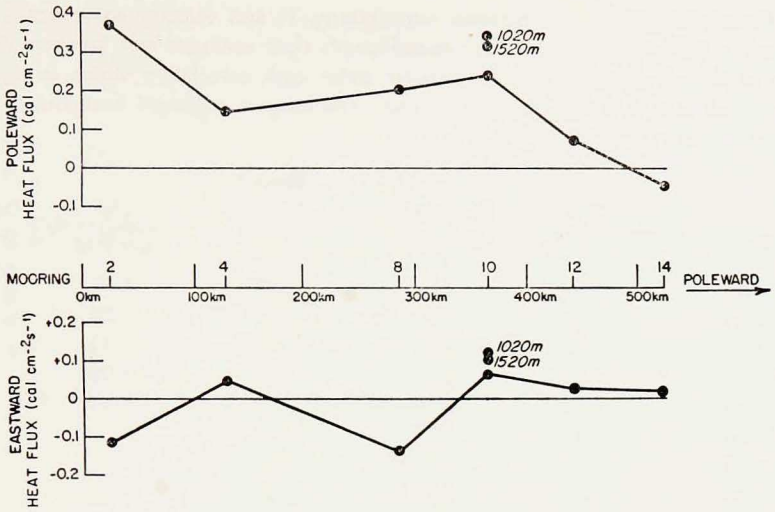

Figure 2. Poleward and eastward heat fluxes due to low-frequency ($\omega < 1$ cycle per day) fluctuations plotted versus meridional position in the Drake Passage. Heat fluxes for the six deep records are connected by lines, while the heat fluxes for the two records at shallower depths on mooring 10 appear as isolated points.

To test whether the heat fluxes due to low-frequency motions are significantly different from zero, cross-correlation coefficients between temperature and velocity components are calculated for each current meter record:

$$C_{uT} = \frac{\overline{u'T'}}{(\overline{u'^2}\,\overline{T'^2})^{\frac{1}{2}}} \qquad C_{vT} = \frac{\overline{v'T'}}{(\overline{v'^2}\,\overline{T'^2})^{\frac{1}{2}}}$$

where $\overline{u'^2}$, $\overline{v'^2}$, and $\overline{T'^2}$ are the variances of eastward velocity, poleward velocity and temperature due to low-frequency motions. To estimate the number of degrees of freedom for these correlation coefficients, the periods of independent sampling for temperature and velocity components at each current meter are estimated from their autocorrelation functions following the method of Davis (1976). Subtracting two (to account for removal of the means) from the quotient of record-length divided by the independent period yields an estimate of the number of degrees of freedom. The correlation coefficients between poleward velocity and temperature on mooring 2 and at 1520 m and 2520 m depths on mooring 10 are significantly different from zero at a 95% confidence level (Table 1). None of the correlation coefficients between eastward velocity and temperature are significant. Because several of the correlations involving poleward heat flux are just below the significance level, overall correlation coefficients are estimated for the measurements near 2700 depth:

Table 1. Correlation coefficients between temperature, T, and velocity components, u (eastward) and v (poleward). Bars denote record-length time averages and brackets denote an average of the six deep records. An asterisk notes each correlation which is significantly different from zero at a 95% confidence level. The average poleward heat flux at 2700 m, $\langle \overline{v'T'} \rangle$, is .16 cal cm^{-2} s^{-1}.

Mooring (Depth)	$\frac{\overline{u'T'}}{(\overline{u'^2}\,\overline{T'^2})^{\frac{1}{2}}}$	Degrees of Freedom	Record Length (days)	$\frac{\overline{v'T'}}{(\overline{v'^2}\,\overline{T'^2})^{\frac{1}{2}}}$	Degrees of Freedom
2 (2770 m)	−.14	51	288	+.43*	62
4 (3100 m)	+.11	34	340	+.22	33
8 (2750 m)	−.24	17	348	+.32	20
10 (1020 m)	+.09	22	226	+.38	15
(1520 m)	+.11	34	349	+.45*	27
(2520 m)	+.18	33	349	+.53*	24
12 (2600 m)	+.17	28	251	+.35	20
14 (2670 m)	+.09	36	328	−.26	27

$$\hat{C}_{uT} = \frac{\langle \overline{u'T'} \rangle}{(\langle \overline{u'^2} \rangle \langle \overline{T'^2} \rangle)^{\frac{1}{2}}} = \frac{-.014}{.613} = -.02$$

$$\hat{C}_{vT} = \frac{\langle \overline{v'T'} \rangle}{(\langle \overline{v'^2} \rangle \langle \overline{T'^2} \rangle)^{\frac{1}{2}}} = \frac{+.16}{.659} = +.25\,*$$

$$\hat{C}_{uT} = \frac{\langle \overline{u'T'} \rangle}{(\langle \overline{u'^2} \rangle \langle \overline{T'^2} \rangle)^{\frac{1}{2}}} \qquad \hat{C}_{vT} = \frac{\langle \overline{v'T'} \rangle}{(\langle \overline{v'^2} \rangle \langle \overline{T'^2} \rangle)^{\frac{1}{2}}}$$

where the brackets denote an average of the six deep decords. Because measurements on different moorings were found to be uncorrelated (Bryden and Pillsbury, 1977), the number of degrees of freedom for these overall correlations is calculated by summing the degrees of freedom for the individual records. The overall correlation coefficient involving eastward heat fluxes, $\hat{C}_{uT} = -.02$, is not significant. The overall correlation coefficient involving poleward heat fluxes, $\hat{C}_{vT} = .25$, is above the 95% confidence level of .09. Thus, the poleward heat flux due to low-frequency motions at 2700 m depth in Drake Passage is significant.

To determine the frequencies of the low-frequency motions which transport heat poleward, a cospectrum of poleward velocity versus temperature is calculated for each current meter record (Fig. 3). The values of these cospectra are directly proportional to the poleward heat flux and the area under the curve in each frequency band is proportional to the heat flux in that band. The cospectra for records on moorings 8, 10, and 12 indicate that the heat fluxes may occur predominantly in two separate bands in the frequency range 0.01 to 0.1 cycles per day (cpd). These bands may be tentatively identified as 0.01 to 0.04 cpd and 0.5 to 0.1 cpd. The poleward heat flux at mooring 4, which appears to have been deployed in a canyon

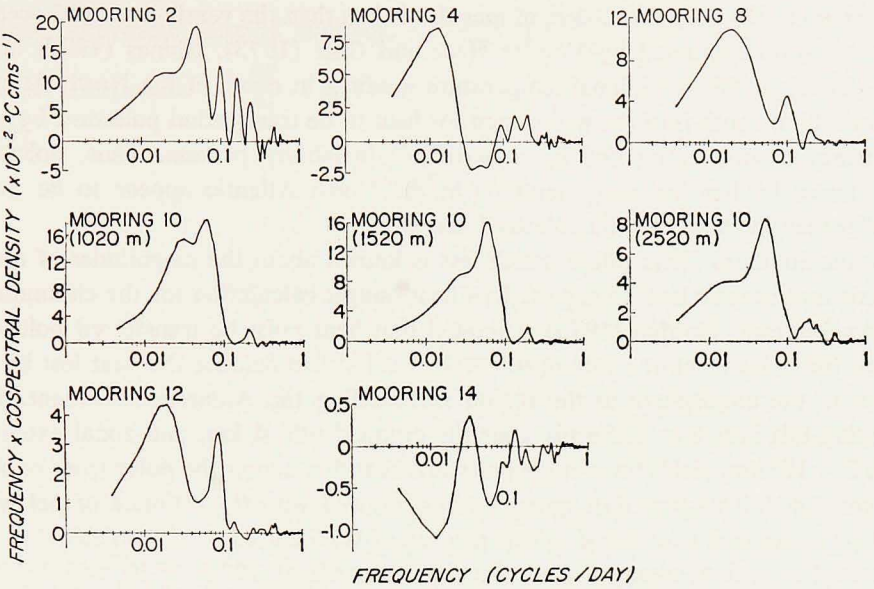

Figure 3. Cospectrum between poleward velocity and temperature for each of the eight records. Positive values represent poleward heat fluxes. Cospectral values multiplied by frequency on a linear scale are plotted versus frequency on a logarithmic scale to emphasize lower frequencies and to make the area under the curve in each frequency band (center frequency = f, bandwidth = $.61f$, $1.39f$) proportional to the heat flux in that band. Cospectra are calculated after the measurements are put through a low-pass filter.

(Pillsbury, Whitworth, Nowlin and Sciremammano, 1979), is due primarily to fluctuations with frequencies less than 0.2 cpd. Most of the poleward heat flux at mooring 2, which had relatively more energetic fluctuations at higher frequencies than other records, is still due to motions of frequencies less than 0.1 cpd although poleward heat fluxes are contributed by motions with frequencies as high as 0.3 cpd. Even at mooring 14 where the net meridional heat flux was equatorward, most of the heat flux occurs at frequencies less than 0.1 cpd. Thus, fluctuations with frequencies lower than 0.1 cpd, that is with periods longer than 10 days, contribute most of the poleward heat transport for all current meter records in the Drake Passage.

Vonder Haar and Oort (1973) have shown that poleward heat flux by the ocean is an important process in the maintenance of heat balance for the combined ocean-atmosphere system in the Northern Hemisphere. Suggestions for the mechanism of poleward heat flux in the ocean include transport by the mean circulation, transport in surface Ekman layers, and transport by low-frequency motions. Estimates of poleward heat transport by low-frequency motions in the western North Atlantic by

Richman (1976) were two orders of magnitude less than the yearly-averaged oceanic heat transport estimated by Vonder Haar and Oort (1973). Rhines (1977) noted that the large-scale meridional temperature gradient in much of the North Atlantic below 200 m depth is of the wrong sign for heat to be transported poleward by low-frequency motions generated by a baroclinic instability process. Thus, poleward heat fluxes by low-frequency motions in the North Atlantic appear to be much smaller than the total oceanic poleward heat flux.

In the Southern Hemisphere, much less is known about the magnitudes of atmospheric and oceanic heat transport. In a heat budget calculation for the circumpolar region, however, Gordon (1975) estimated that heat must be transferred poleward across the polar front at a rate of 9.5×10^{13} cal s^{-1} to balance the heat lost by the ocean to the atmosphere in the region surrounding the Antarctic continent. Distributing this heat flux uniformly over the ocean depth, 4 km, and zonal extent at 60S, 2×10^4 km, yields an average poleward heat flux across the polar front of 0.12 cal cm^{-2} s^{-1}. This heat flux agrees reasonably well with the estimate of poleward heat flux averaged over the six deep records of 0.16 cal cm^{-2} s^{-1} (Table 1). The poleward heat flux averaged over the three records at 1020, 1520 and 2520 m depths on mooring 10, which is in the region of the polar front, is 0.29 cal cm^{-2} s^{-1} which is a factor of 2.4 larger than the distributed heat flux. While the Drake Passage region may not be typical of the circumpolar region, the magnitude of the observed heat fluxes suggests that poleward heat flux by the low-frequency motions makes a major contribution to the oceanic heat flux in the circumpolar region.

Gordon (1975) extended his heat budget to estimate the northward transport of Antarctic Bottom Water across the Polar Front by assuming that lateral diffusion across the polar front was small. He required a northward transport of cold (2.7°C colder than modal deep water) Antarctic Bottom Water of 38×10^6 m^3 s^{-1} to balance the 9.5×10^{13} cal s^{-1} of heat lost by the ocean to the atmosphere south of the polar front. The observed heat fluxes, however, suggest that lateral diffusion across the Polar Front is important and that low-frequency fluctuations transport much of the heat across the Polar Front without a net transport of water. If these heat fluxes observed in Drake Passage are typical of the circumpolar region, Gordon's estimate of northward transport of Antarctic Bottom Water must be greatly reduced.

3. Poleward heat flux and conversion of available potential energy

Poleward heat fluxes in the circumpolar region, where horizontal temperature gradients are directed equatorward, are associated with conversion of available potential energy contained in the large-scale density distribution into eddy kinetic and potential energies. The equation representing this transfer is derived from the momentum equations and the equation for the conservation of heat. Linearizing these equations about a mean eastward current, $\bar{U}(z)$, which is in geostrophic balance with

a mean northward pressure gradient, $\frac{\partial \bar{p}}{\partial y}$, and about a mean vertical gradient of potential temperature, $\frac{\partial \theta}{\partial z}$, and neglecting terms involving friction and diffusion yields:

$$\left(\frac{\partial}{\partial t} + \bar{U}\frac{\partial}{\partial x}\right) u' - f v' = -\frac{\partial p'}{\rho_0 \partial x} \tag{1a}$$

$$\left(\frac{\partial}{\partial t} + \bar{U}\frac{\partial}{\partial x}\right) v' + f u' = -\frac{\partial p'}{\rho_0 \partial y} \tag{1b}$$

$$O = -\frac{\partial p'}{\partial z} - g\rho' \tag{1c}$$

$$\left(\frac{\partial}{\partial t} + \bar{U}\frac{\partial}{\partial x}\right) T' + v'\frac{\partial \bar{T}}{\partial y} + w'\frac{\partial \bar{\theta}}{\partial z} = 0 \tag{1d}$$

where bars denote time-averaged values, primes denote deviations from time-averaged values, $f = -f_0 + \beta y$ is the Coriolis parameter, g is the gravitational acceleration, w is vertical velocity and ρ is the density of seawater. Because of the correlation between temperature and salinity, density can be considered a function of temperature alone, $\rho = \rho_0 - \alpha T$ so that fluctuations in density are directly related to fluctuations in temperature $\rho' = -\alpha T'$. Multiplying (1a) by $\rho_0 u'$, (1b) by $\rho_0 v'$ and (1c) by w', adding the 3 equations and averaging and multiplying (1d) by $g\alpha\left(\frac{\partial \bar{\theta}}{\partial z}\right)^{-1} T'$ and averaging yields 2 equations:

$$\left(\frac{\partial}{\partial t} + \bar{U}\frac{\partial}{\partial x}\right) \rho_0 \left(\frac{\overline{u'^2} + \overline{v'^2}}{2}\right) = -\left(\overline{u'\frac{\partial p'}{\partial x}} + \overline{v'\frac{\partial p'}{\partial y}} + \overline{w'\frac{\partial p'}{\partial z}}\right) + g\alpha\,\overline{w'T'} \tag{2a}$$

$$\left(\frac{\partial}{\partial t} + \bar{U}\frac{\partial}{\partial x}\right) \frac{g\alpha\,\overline{T'^2}}{2\left(\frac{\partial \bar{\theta}}{\partial z}\right)} = -\frac{g\alpha}{\left(\frac{\partial \bar{\theta}}{\partial z}\right)} \overline{v'T'}\,\frac{\partial \bar{T}}{\partial y} - g\alpha\,\overline{w'T'}. \tag{2b}$$

Adding these equations and integrating over a fluid volume V with surface area S and using the continuity equation, $\frac{\partial u'}{\partial x} + \frac{\partial v'}{\partial y} + \frac{\partial w'}{\partial z} = 0$, and the divergence theorem yields:

$$\int dV \left(\frac{\partial}{\partial t} + \bar{U}\frac{\partial}{\partial x}\right)\left[\rho_0\left(\frac{\overline{u'^2} + \overline{v'^2}}{2}\right) + \frac{g\alpha\,\overline{T'^2}}{2\left(\frac{\partial \bar{\theta}}{\partial z}\right)}\right]$$

$$= -\int dV\,\frac{g\alpha}{\left(\frac{\partial \bar{\theta}}{\partial z}\right)} \overline{v'T'}\,\frac{\partial \bar{T}}{\partial y} - \int dS\,\overrightarrow{p'u'} \cdot \vec{n}. \tag{3}$$

Following the definitions of Lorenz (1967), $\rho_0 \frac{\overline{u'^2} + \overline{v'^2}}{2}$ is identified as eddy kinetic energy, $\frac{g\alpha\,\overline{T'^2}}{2\left(\frac{\partial\bar{\theta}}{\partial z}\right)}$ as eddy potential energy and $-g\alpha \frac{\overline{v'T'}}{\frac{\partial\bar{\theta}}{\partial z}} \frac{\partial\bar{T}}{\partial y}$ as the conversion of available potential energy. If the fluid volume is chosen so that $\vec{u'} \cdot \vec{n}$ is zero everywhere on its boundary or if the pressure work term on the boundary is negligible, that is, $\int dS\, \overline{p'\,\vec{u'} \cdot \vec{n}}$ is small, then poleward heat flux, $\overline{v'T'} < 0$, in a region of equatorward temperature gradient, $\frac{\partial\bar{T}}{\partial y} > 0$, results in a positive conversion of available potential energy and a growth, $\frac{\partial}{\partial t} + \bar{U}\frac{\partial}{\partial x} > 0$, of eddy kinetic plus eddy potential energy.

To estimate the conversion of available potential energy at 2700 m in Drake Passage, the thermal wind relation $\rho_0 f \frac{\partial\bar{U}}{\partial z} = -g\alpha \frac{\partial\bar{T}}{\partial y}$, is used to rewrite the conversion as:

$$\frac{-g\alpha}{\frac{\partial\bar{\theta}}{\partial z}} \overline{v'T'} \frac{\partial\bar{T}}{\partial y} = \frac{\rho_0 f}{\frac{\partial\bar{\theta}}{\partial z}} \overline{v'T'} \frac{\partial\bar{U}}{\partial z}.$$

From hydrographic measurements, the vertical shear of mean velocity at 2700 m is estimated to be $\frac{\partial\bar{U}}{\partial z} = 2.9 \times 10^{-5}$ s^{-1} and the vertical gradient of potential temperature is $\frac{\partial\bar{\theta}}{\partial z} = 0.52 \times 10^{-5}$ °C cm^{-1}. From the average poleward heat flux at 2700 m of 0.16 cal cm^{-2} s^{-1} (Table 1), the rate of conversion of available potential energy is estimated to be 1.2×10^{-4} erg cm^{-3} s^{-1}. Thus, on average at 2700 m depth the available potential energy is converted to eddy kinetic and potential energies at a rate of 10 erg cm^{-3}/day.

To estimate typical time scales for growth of the low-frequency motions in this region, this conversion should be compared with the magnitude of low-frequency kinetic and potential energies. The average kinetic energy, $\rho_0\,(\overline{u'^2} + \overline{v'^2})/2$, and potential energy, $g\alpha\,\overline{T'^2}/2\bar{\theta}_z$, of the low-frequency motions are calculated for each current meter record (Fig. 4). Values of α and $\bar{\theta}_z$ are estimated for each record from nearby hydrographic measurements. At the northern end of the Passage at mooring 2, kinetic energy is a factor of 2 larger than potential energy, while in the southern Passage at moorings 12 and 14 potential and kinetic energies are about the same size. In the central and north-central Passage at moorings 4, 8 and 10, potential energy exceeds kinetic energy by an order of magnitude. Typical values of eddy kinetic and potential energies at 2700 m are estimated to be 41 and 116 erg cm^{-3} respectively by averaging over the six deep records. A typical time scale for the

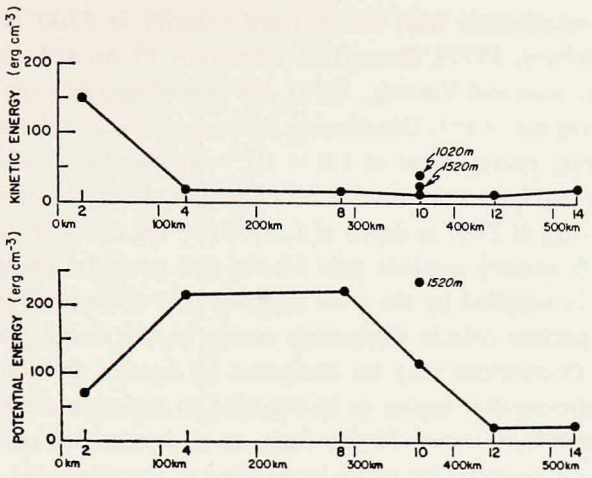

Figure 4. Kinetic energy $\rho_0 \dfrac{\overline{u'^2} + \overline{v'^2}}{2}$ and potential energy $\left(\dfrac{g\,\alpha\,\overline{T'^2}}{2\bar{\theta}_z}\right)$ contained in the low-frequency motions plotted versus meridional position in the Drake Passage. Energies for the six deep records are connected by lines while kinetic energies at 1020 and 1520 m and potential energy at 1520 m on mooring 10 appear as isolated points. Potential energy at 1020 m on mooring 10, 940 erg cm^{-3} is not plotted because it is so large.

fluctuations to grow from zero to their average energy level is estimated to be 15 days by dividing the sum of the typical kinetic and potential energies by the average conversion of available potential energy at 2700 m depth. Consideration of the eddy energies and conversion rates at shallower depths on mooring 10 suggest this time scale may be too short. While the conversion of available potential energy at 1020 m depth is a factor of 2 larger than that at 2520 m, 2.2×10^{-4} versus 1.2×10^{-4} erg cm^{-3} s^{-1}, the potential energy is a factor of 8 larger, 970 versus 125 erg cm^{-3}, and the kinetic energy is a factor of 3 larger, 42 versus 14 erg cm^{-3}, at the shallower depth. Based on the energies and conversion rate at 1020 m depth on mooring 10, a typical time scale for growth of the low-frequency motions is estimated to be 54 days. Since kinetic and potential energies of the entire water column are probably dominated by contributions from shallower depths and since the rate of conversion appears to be constant within a factor of 2 over depth, the longer time scale of 54 days may be a more representative value for the time scale for growth of the low-frequency motions.

To compare this conversion of available potential energy with the rate at which energy is supplied to the water column by wind, the rate of energy input by wind is estimated to be

$$u_s\,\tau^x$$

where u_s is the eastward surface velocity and τ^x is the eastward wind stress. Based

on geostrophic calculations with an eastward velocity at 2700 m of 1.6 cm s^{-1} (Bryden and Pillsbury, 1977), the surface velocity is 17 cm s^{-1}. For $\tau^x = 2$ dynes cm^{-2} at 60S (Evenson and Veronis, 1975), the rate of energy input by wind is estimated to be 34 erg cm^{-2} s^{-1}. Distributing this over a water column depth of 3500 m yields an average energy input of 1.0×10^{-4} erg cm^{-3} s^{-1}. This rate of energy input is smaller than, but of the same order of magnitude as, the conversion of available potential energy at 2700 m depth of 1.2×10^{-4} erg cm^{-3} s^{-1} estimated above.

That the low-frequency motions gain kinetic and potential energies at the same rate that energy is supplied by the wind suggests that these low-frequency motions may play an important role in dissipating energy in the circumpolar regions. The energy of these fluctuations may be dissipated by bottom friction or be radiated away from the circumpolar region or be recycled to maintain the kinetic energy of the mean Circumpolar Current. In any case, an understanding of the dynamics of these fluctuations is essential for an understanding of the energetics of the Antarctic Circumpolar Current.

4. Comparison of observations with a baroclinic instability model

Conversion of available potential energy into eddy potential and kinetic energies under certain conditions is the primary prediction of the baroclinic instability model. The usefulness of this model for large-scale modeling of the ocean or atmosphere arises from its prediction of specific dependences of eddy heat, momentum and vorticity fluxes on large-scale gradients of temperature and vorticity (Green, 1970). As a result, the effects of eddies can then be parameterized in terms of large-scale distributions without resolving the eddies explicitly. It is debatable, however, whether the linearized, small amplitude baroclinic instability model should be applied to observations of large amplitude oceanic eddies. On the one hand, this model assumes the presence of a mean circulation on which infinitesimal amplitude eddies grow while in the ocean eddy velocities and mean flow of comparable magnitudes coexist. The interaction of oceanic eddies and mean flow then could be very different from that in the simple model. On the other hand, judicious analysis of atmospheric observations has shown that heat, momentum and vorticity transports are similar to those suggested by the linearized instability model (Green, 1970; Stone, 1974). In this section the observations in Drake Passage are compared with the linearized baroclinic instability model to assess the applicability of this model for describing the energy conversion process.

A necessary condition for the baroclinic instability process to occur was derived by Charney and Stern (1962) from consideration of the imaginary part of the equation for enstrophy conservation:

$$\int_{-H}^{0} Q_y \frac{\psi^2}{(\bar{U}-c)^2}\,dz + \frac{f^2}{N^2}\frac{\bar{U}_z}{(\bar{U}-c)^2}\psi^2\Big|_{z=0} - \frac{f^2}{N^2}\frac{\bar{U}_z}{(\bar{U}-c)^2}\psi^2\Big|_{z=-H} = 0 \tag{4}$$

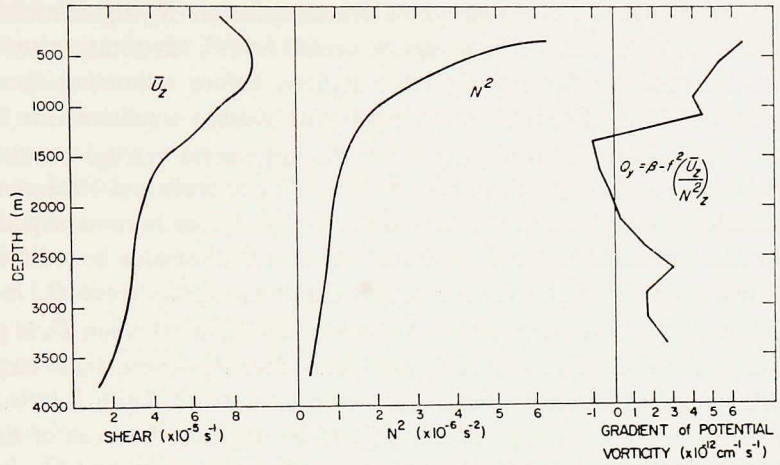

Figure 5. Vertical shear of eastward velocity, $\bar{U}_z$, Brunt-Väisälä frequency squared, N^2, and meridional gradient of potential vorticity, $Q_y = \beta - f^2\left(\frac{\bar{U}_z}{N^2}\right)_z$, plotted versus depth. $\bar{U}_z$ is the geostrophic velocity shear estimated from hydrographic stations at the north and south sides of Drake Passage. N^2 is estimated from an average of five hydrographic stations near mooring 10 in the middle of the Passage. Q_y is estimated from $\bar{U}_z$ and N^2 by taking differences between values of $\bar{U}_z/N^2$ separated by 250 m depth intervals. Values of f, -1.25×10^{-4} s^{-1}, and β, 1.18×10^{-13} cm^{-1} s^{-1} are for a latitude of 59S.

where ψ is the streamfunction for the fluctuation velocity field, N is the Brunt-Väisälä frequency, c is the phase speed of the fluctuations, H is the depth of water, and Q_y is the meridional gradient of potential vorticity, $Q_y = \beta - f^2\left(\frac{\bar{U}_z}{N^2}\right)_z$. Since f^2, N^2, ψ^2, $(U-c)^2$ are positive definite, this necessary condition can be rewritten as three conditions for instability (Gill, Green and Simmons, 1974):

(a) Q_y change sign between $z = 0$ and $-H$.

or

(b) $\bar{U}_z$ at $z = 0$ have sign opposite that of Q_y.

or

(c) $\bar{U}_z$ at $z = -H$ have the same sign as Q_y.

To examine these conditions in the Drake Passage, U_z, N^2 and Q_y were calculated from hydrographic measurements (Fig. 5). Hydrographic stations at the north and south ends of the Passage are used to calculate geostrophically the vertical shear of eastward current, $\bar{U}_z$. Estimates of N^2 from individual hydrographic stations caused wild variability in vertical profiles of Q_y. Because the three current meter records on mooring 10 provide all of the information on vertical variability of the low-frequency

motions, N is estimated from hydrographic measurements in the central Passage near mooring 10. To obtain a slowly varying profile for N^2, temperature and salinity values are averaged for five hydrographic stations before estimating the vertical density gradient. Thus, the profile of N^2 represents average conditions for the local region near mooring 10, while $\bar{U}_z$ represents the large-scale average conditions for the entire Drake Passage. Q_y, then, is a mixture of large-scale and local conditions. Q_y is generally positive in the water column although it does become slightly negative for depths between 1200 and 1800 m. This profile illustrates how difficult it is to satisfy instability condition (a) for eastward current shears since Q_y is usually dominated by vertical variations in N^2. To satisfy condition (a) when $\bar{U}_z$ is positive, $\bar{U}_{zz}/\bar{U}_z$ must be greater than N_z/N. In the Drake Passage where $\bar{U}_z$ is large compared with typical mid-ocean values, there is only a small depth interval where $\bar{U}_{zz}/\bar{U}_z$ exceeds N_z/N by enough to cause Q_y to be negative. Because of the peculiar mixture of local and large-scale averaging involved in estimating Q_y, it is possible that Q_y is nonnegative at all depths. The overall impression from the distribution of density across the Passage (Fig. 1) is that the slope of the isopycnals increases as the depth increases which would imply that Q_y is always positive. Thus, whether or not instability condition (a) is satisfied is debatable. It appears that near mooring 10 Q_y does change sign and takes on small negative values but only over a limited depth interval between 1200 and 1800 m. Since both Q_y and $\bar{U}_z$ are positive near the surface, condition (b) is not satisfied. Since Q_y and $\bar{U}_z$ are also positive at the ocean bottom, the instability condition (c) is satisfied. de Szoeke (1977) pointed out that condition (c) is satisfied in Drake Passage and suggested that because Q_y appeared to be positive at all depths the vertical shear of eastward velocity at the bottom boundary must be the principal destabilizing influence for generating low-frequency motions in the Drake Passage.

If the instability process were due only to the change of sign of Q_y, from generally positive values to small negative values in a limited depth interval, the fluctuations would necessarily be small or of limited vertical extent so that

$$\int Q_y \frac{\psi^2}{(\bar{U}-c)^2}\, dz = 0.$$

Because of the effect of the bottom boundary, which gives rise to condition (c), the fluctuations can have larger amplitude throughout the water column since the contribution from generally positive values of

$$Q_y \frac{\psi^2}{(\bar{U}-c)^2}$$

in the interior of the water column is balanced by the contribution from the bottom boundary:

$$\frac{f^2}{N^2} \frac{\bar{U}_z \psi^2}{(\bar{U}-c)^2} \Bigg| z = -H.$$

Thus, even though Q_y may change sign in a limited depth interval, the baroclinic instability process in the Drake Passage is primarily due to the presence of shear at the bottom boundary.

Since the necessary condition for instability is satisfied and since the fluctuations do convert available potential energy, it is appropriate to compare these observations with the baroclinic instability model. The model of Gill, Green and Simmons (1974) is chosen for initial comparison because it includes continuous vertical variations in contrast to the two-layer model of Robinson and McWilliams (1974). Because Gill, Green and Simmons suggested that a vertical phase shift is a signature of the instability process, comparisons of the model are made principally with the observations on mooring 10 which had current and temperature records at 1020, 1520, and 2520 m depths.

For the Gill, Green and Simmons model, which assumes a stream-function, ψ, for the fluctuations of the form

$$\psi = A\,(z)\exp\,(kc_i t)\cos\,[k(x-c_r t) + \phi(z)] \tag{5}$$

where k is the zonal wavenumber, $c = c_r + ic_i$ is the phase speed, and $\phi(z)$ is the vertical phase function, conversion of available potential energy occurs when $k\,\bar{U}_z\,\phi_z$ is negative. For their examples of instability ϕ_z was such that events occur earlier at greater depths where energy conversion is taking place.[2] To determine whether such a vertical phase function exists in these observations, plots of temperature and velocity components versus time are compared for three depths at mooring 10 (Fig. 6). Temperatures change simultaneously at the three depths. For both eastward and poleward velocities, the deeper velocities appear to lead the shallower velocities by periods of order 1 day. The lack of a phase lag in temperature, while it does not rule out a vertical phase function provided the amplitude, $A(z)$, and phase are related by $\tan(-\phi(z)) = A\phi_z/A_z$, warns that the absence of a vertical phase shift does not rule out the occurrence of baroclinic instability. The vertical phase shifts in velocity components are consistent with the predicition of the Gill, Green and Simmons model.

To investigate the mechanism by which the energy transfer takes place in the Drake Passage, squared coherence and phase are calculated versus frequency for the time series recorded on mooring 10. Because the squared coherence generally has a maximum in the frequency band 0.058 to 0.068 cpd and because conversion of available potential energy, shown by positive values of the cospectra between

2. Care in the choice of sign convention is essential to an interpretation of the phase function $\phi(z)$. Gill, Green and Simmons maintain positive k and allow $\omega = kc_r$ to change sign with $\bar{U}$. In this work, ω remains positive and k changes sign with $\bar{U}$. The difference arises in the sign of ϕ_z which Gill, Green and Simmons state is negative while here ϕ_z must be generally positive to ensure that $k\,\bar{U}_z\phi_z > 0$ since $k\,\bar{U}_z$ is positive if $\bar{U}_z$ has the same sign as $\bar{U}$. The net result of either convention is identical, i.e., for energy conversion to occur, upward phase propagation is necessary so that events occur earlier at greater depths.

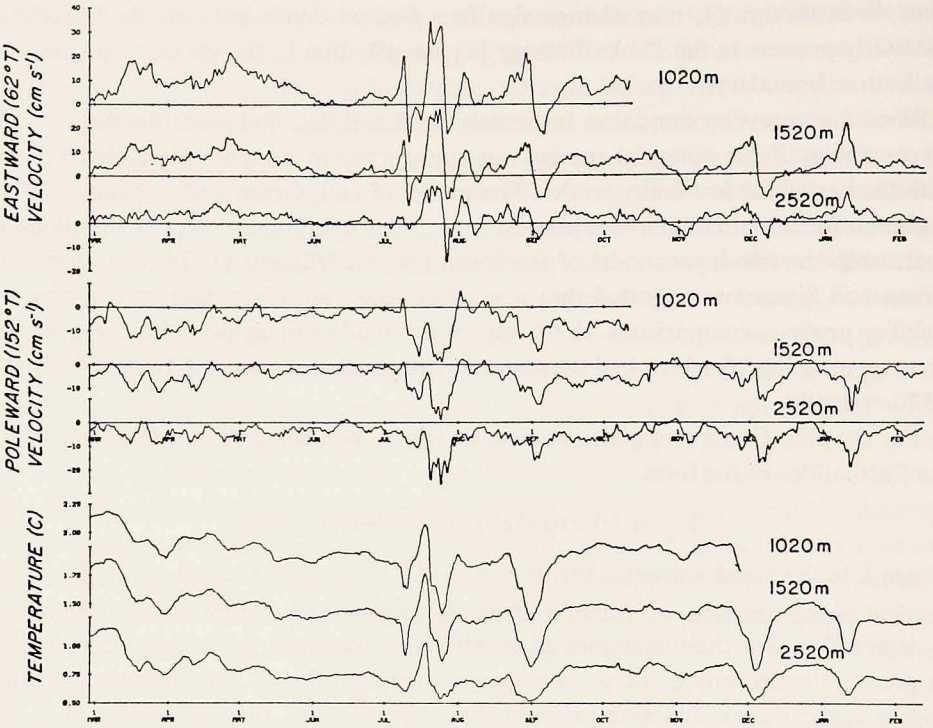

Figure 6. Eastward velocity, poleward velocity and temperature plotted versus time for the three records at 1020, 1520 and 2520 m depths on mooring 10. The time series have been put through a low-pass filter with half-power at a period of 40 hours to eliminate high-frequency motions.

poleward velocity and temperature (Fig. 3) occurs in this band, the phases in this frequency band (Table 2) are used to estimate the form of the streamfunction for comparison with the model streamfunction of Gill, Green and Simmons. As noted for the time series (Fig. 6), temperatures are virtually in phase at all depths, while eastward and poleward velocities at 2520 m lead velocities at 1020 m by about 35°. At all three depths there is a consistent phase difference between eastward and poleward velocities such that poleward velocity leads eastward velocity by about 70°. This phase difference between velocity components was first suggested by the dominance of energy in the counterclockwise half of the rotary spectrum. The ratio of energy in the counterclockwise spectrum to that in the clockwise spectrum, S^{++}/S^{--}, is greater than 3 for each of the records on mooring 10 (Table 2). Temperature leads eastward velocity by about 90° at 1020 and 1520 m but only by 45° at 2520 m depth. Most importantly, temperature and poleward velocity are nearly in phase at all three depths with temperature leading poleward velocity by only 26° at 1020 m and poleward velocity leading temperature by 28° at 2520 m.

Table 2. Coherence squared and phase difference between measured variables (u = eastward velocity, v = poleward velocity, T = temperature) at three depths (1 = 1020 m, 2 = 1520 m, 3 = 2520 m) on mooring 10 in the frequency band 0.058-0.068 cpd. Averaging is done effectively over about 4 frequency bands. Positive phase difference means the maximum in series 2 precedes the maximum in series 1. Ratios of counterclockwise energy to clockwise energy, S^{++}/S^{--}, and of eastward energy to poleward energy, S^{uu}/S^{vv}, are also presented for the three depths in this frequency band.

	Coherence Squared	Phase
$u_1 \times u_2$	.99	8°
$u_2 \times u_3$	.91	27°
$u_1 \times u_3$	.89	36°
$v_1 \times v_2$	.95	9°
$v_2 \times v_3$	.89	24°
$v_1 \times v_3$	.75	34°
$T_1 \times T_2$	.97	−1°
$T_2 \times T_3$	.91	−6°
$T_1 \times T_3$	.84	−7°
$u_1 \times T_1$	.84	102°
$u_2 \times T_2$	.64	92°
$u_3 \times T_3$	.40	45°
$v_1 \times T_1$	.54	26°
$v_2 \times T_2$	.61	17°
$v_3 \times T_3$	.57	−28°
$u_1 \times v_1$	.56	72°
$u_2 \times v_2$	.59	72°
$u_3 \times v_3$	.60	63°
$S_1^{++}/S_1^{--} = 3.7$	$S_1^{uu}/S_1^{vv} = 3.9$	
$S_2^{++}/S_2^{--} = 4.5$	$S_2^{uu}/S_2^{vv} = 2.9$	
$S_3^{++}/S_3^{--} = 4.9$	$S_3^{uu}/S_3^{vv} = 1.7$	

Because the observations indicate a 70° phase difference between eastward and poleward velocities, proportional to $-\psi_y$ and ψ_x respectively, a fit of these observations to the model streamfunction (5) which requires eastward and poleward velocities to be in phase is hopeless. The observed 70° phase difference suggests that a more appropriate form for a model streamfunction is:

$$\psi = A(x,z)\cos(ly - \omega t + \phi(z)) \tag{6}$$

since a 70° phase difference is close to the 90° phase difference between velocity components for this streamfunction. That temperature, proportional to $-\psi_z$, and eastward velocity have a phase difference of about 90° while temperature and poleward velocity are nearly in phase suggests that the amplitude, A, is a function of x rather than y. Because the temperature variance is larger at shallower depths, A and A_z must have the same sign. That eastward velocity lags temperature by about 90° suggests the phase velocity, ω/l, is directed equatorward. That poleward velocity leads eastward velocity then suggests that A_x is positive.

Several models in which velocity components are 90° different in phase have been investigated. Yao (1977) studied waves forced by wind in the Drake Passage, which he modeled as a channel with depth decreasing to the east. Yao found waves trapped to the topography so their streamfunction amplitudes increase to the east as suggested by the model streamfunction (6). These waves, however, propagate in the poleward direction in contrast to the equatorward propagation suggested by the 90° phase differences between eastward velocity and temperature. More importantly, Yao did not investigate the stability of these waves so his model waves do not grow and they cannot explain the observed conversion of available potential energy.

In comparing observations in the Denmark Strait overflow with a baroclinic instability model, Smith (1976) found a 90° phase difference between velocity components. Because his instability model was designed for a channel, Smith's growing wave had a streamfunction amplitude which varied across the channel. While the Drake Passage might be modeled as a channel with northern and southern walls at South America and Antarctica respectively, the phase differences suggest that the streamfunction amplitude varies in the along-channel rather than cross-channel direction. In Smith's model then, temperature and cross-channel velocity are nearly 90° out of phase and temperature and along-channel velocity are nearly in phase, while in Drake Passage temperature and poleward (cross-channel) velocity are nearly in phase and temperature and eastward (along-channel) velocity are nearly 90° out of phase. In agreement with the results for Drake Passage, Smith found that the instability was due to the vertical shear of mean velocity near the bottom and was unable to detect any vertical phase difference in the observations in the Denmark Strait.

Hogg (1976) investigated spatially growing baroclinic waves which grow by conversion of available potential energy but which have shorter wavelengths than the more commonly studied temporally growing waves. Because Bryden and Pillsbury (1977) found the fluctuations in Drake Passage to be uncorrelated over horizontal separations of 80 km, the short wavelength of spatially growing waves is consistent with the observations. These waves also grow in the direction of the mean flow. Since the mean flow is eastward in Drake Passage and since the model streamfunction amplitude is found to increase eastward, again the observations are consistent with spatially growing waves. The major disagreement between these waves and the observations is the depth range over which energy conversion occurs. Hogg (1976) found the conversion to occur only over a limited depth interval near the critical level where Q_y changes sign, while the observations show energy conversion occurring at least between 1020 m and 2520 m depths at mooring 10. This disagreement might be reconciled in a model of spatially growing waves for which the shear at the bottom boundary is the principal destabilizing influence, as found above for the Drake Passage observations, instead of the interior critical level in Hogg's model. Of these three models which predict a 90° phase difference between velocity com-

ponents, the most promising is that of Hogg (1976) since it predicts growth of fluctuations by conversion of available potential energy, short spatial scales for the fluctuations, and growth in the direction of the mean flow, all of which are consistent with the observations.

In addition to comparing these observations with specific baroclinic instability models, the dependence of heat fluxes on large scale gradients of temperature, which is suggested by the instability theory, can be estimated from these observations. Green (1970) showed that for a baroclinic instability process heat fluxes due to low-frequency motions should be proportional to the large-scale gradient of temperature:

$$\overline{v'T'} \propto \left(\frac{\partial T}{\partial y}\right)^2 \Big/ \frac{\partial \bar{\theta}}{\partial z} . \tag{7}$$

By making an additional assumption that the amplitude of the fluctuations is equal to the magnitude of the mean flow, Stone (1972, 1974) derived a parameterization where even the constant of proportionality was determined:

$$\overline{v'T'} = -.144 \frac{gH^2}{f^2 T}\left(\frac{g}{T}\frac{\partial \bar{\theta}}{\partial z}\right)^{\frac{1}{2}} \left|\frac{\partial T}{\partial y}\right| \frac{\partial T}{\partial y} . \tag{8}$$

Stone found that this parameterization agreed remarkably well with the results of Green who fit his expression (7) to observed values of atmospheric heat transport to determine the proportionality constant. For the ocean where density is a function of salinity as well as temperature, Stone's parameterization (8) can be written in the form:

$$\overline{v'T'} = \frac{CH^2N}{f} |\bar{U}_z| \frac{\partial T}{\partial y} . \tag{9}$$

For values of $\overline{v'T'} = 0.16$°C cm s^{-1}, $\bar{U}_z = 2.9$ cm s^{-1} km^{-1}, $\partial\bar{T}/\partial y = 2.6 \times 10^{-3}$°C km^{-1}, and $N = .77 \times 10^{-3}$ s^{-1} at 2700 m depth in the Drake Passage and with H taken to be the average depth, 3.5 km, C can be estimated to be 0.28 which is to be compared with Stone's value $C = 0.144$. Such agreement within a factor of 2 must be considered encouraging in view of the use of values typical of only one depth. Because values of $\bar{U}_z$, $\partial\bar{T}/\partial y$ and N determined from hydrographic data are all a factor of 2 larger at 1020 m than at 2520 m depth while the poleward heat flux, $\overline{v'T'}$, increases by less than a factor of 2 between 2520 and 1020 m depth on mooring 10, this estimate of $C = 0.28$ is likely to be larger than a value of C determined for the entire water column. The agreement with atmospheric results within a factor of 2 suggests that parameterization of heat fluxes due to low-frequency motions in terms of large-scale gradients of temperature may be useful in numerical models of large-scale ocean circulation.

5. Conclusions

From eight year-long records of current and temperature measured in the Drake Passage during 1975, heat fluxes are estimated for low-frequency ($\omega < 1$ cpd) fluctuations. Correlation coefficients between poleward velocity and temperature are generally positive and three of eight correlations are significant at the 95% confidence level. An average correlation coefficient for the six deep records near 2700 m depth is significantly positive. Cospectra between poleward velocity and temperature show that most of the poleward heat flux is due to motions with periods longer than 10 days. If the average poleward heat flux at 2700 m depth of 0.16°cal cm^{-2} s^{-1} is typical of heat flux values in the circumpolar region, the low-frequency motions transport enough heat poleward across the polar front without a net mass transport to balance the heat lost to the atmosphere by waters around the Antarctic continent which was estimated by Gordon (1975) to be 9.5×10^{13} cal s^{-1}. If these motions do transport such large amounts of heat poleward, the northward transport of Antarctic Bottom Water must be greatly reduced from Gordon's value of 38×10^6 m^3 s^{-1} based on a heat budget calculation which did not include an estimate of the poleward heat flux due to low-frequency fluctuations.

Because there is a large-scale equatorial temperature gradient in Drake Passage, poleward fluxes are associated with a conversion of available potential energy contained in this large-scale density distribution into kinetic and potential energies of the low-frequency motions. At 2700 m depth, this conversion is estimated to occur at a rate of 1.2×10^{-4} erg cm^{-3} s^{-1}, which is about the same size as the rate of input of energy by wind averaged over the depth of the water column.

Because the conversion of available potential energy is the primary prediction of baroclinic instability theory, these observations are compared with this theory. In terms of the necessary condition for instability first derived by Charney and Stern (1962), the vertical shear of eastward velocity at the bottom boundary is the principal destabilizing influence in the Drake Passage. The vertical phase function, which was suggested by Gill, Green and Simmons (1974) as a possible signature of the instability process, is difficult to detect in these measurements. While small phase differences of approximately 35° over 1500 m depth are found in velocity components with deeper velocities leading shallower velocities, no phase difference over 1500 m depth is found in temperature. A clearer signature of the instability process in these observations is that temperature and poleward velocity are nearly in phase. Associated with this signature are a phase difference of about 70° between poleward and eastward velocity components and a dominance of energy in the counterclockwise half of the rotary spectra. The observations seem to be consistent with a model of spatially growing baroclinic waves investigated by Hogg (1976). Finally, the dependence of heat fluxes due to low-frequency motions on large-scale temperature gradients, which is suggested by the instability theory and has been

tested with atmospheric measurements by Green (1970) and Stone (1974), is found to agree with results for the atmosphere within a factor of 2.

These results indicate that the low-frequency current and temperature fluctuations have a profound effect on the mean circulation in the circumpolar region. They act to transport heat poleward at the same rate the waters around the Antarctic continent lose heat to the atmosphere. At the same time, they convert available potential energy into eddy potential and kinetic energies at the same rate the wind puts energy into the water column. The processes which cause the fluctuations to lose their energy are likely to be the processes which ultimately dissipate the energy supplied by the wind in the circumpolar region. Thus, an understanding of the processes which cause the fluctuations to lose their energy is essential to an understanding of the dynamics of the Antarctic Circumpolar Current.

Acknowledgments. This work was supported by the Office of the International Decade of Ocean Exploration of the National Science Foundation under grants OCE76-80066 to Oregon State University and OCE 77-22887 to Woods Hole Oceanographic Institution. The measurements were made by the Oregon State University Buoy Group under the direction of Dale Pillsbury. The quality of the measurements is due to the carefulness of Robert Still in preparing the instruments for deployment. Dennis Root and Joseph Bottero processed the data and did the calculations reported here. Worth Nowlin and Thomas Whitworth provided their hydrographic measurements prior to publication. Roland de Szoeke explained the intricacies of baroclinic instability theory and pointed out the importance of the vertical shear at the bottom as a destabilizing influence. The paper is Contribution No. 4099 of the Woods Hole Oceanographic Institution.

REFERENCES

Bernstein, R. L., and W. B. White. 1974. Time and length scales of baroclinic eddies in the central North Pacific Ocean. J. Phys. Oceanogr., *4,* 613–624.

Bryden, H. L., and R. D. Pillsbury. 1977. Variability of deep flow in the Drake Passage from year-long current measurements. J. Phys. Oceanogr., *7,* 803–810.

Charney, J. G., and M. E. Stern. 1962. On the stability of internal baroclinic jets in a rotating atmosphere. J. Atm. Sci., *19,* 159–172.

Davis, R. E. 1976. Predictability of sea surface temperature and sea level pressure anomalies over the North Pacific Ocean. J. Phys. Oceanogr., *6,* 249–266.

de Szoeke, R. A. 1977. A model of baroclinic instability in the Southern Ocean (Abstract). EOS, Trans. Am. Geophys. Un., *58,* 1168.

Eady, E. T. 1949. Long waves and cyclone waves. Tellus, *1,* 33–52.

Evenson, A. J., and G. Veronis. 1975. Continuous representation of wind stress and wind stress curl over the world ocean. J. Mar. Res., *33* (*Suppl.*), 131–144.

Gill, A. E., J. S. A. Green, and A. J. Simmons. 1974. Energy partition in the large-scale ocean circulation and the production of mid-ocean eddies. Deep-Sea Res., *21,* 499–528.

Gordon, A. L. 1975. General ocean circulation. Numerical Models of Ocean Circulation. National Academy of Sciences, Washington, D.C., 364 pp.

Gould, W. J., W. J. Schmitz, Jr., and C. Wunsch. 1974. Preliminary field results for a Mid-Ocean Dynamics Experiment (MODE-O). Deep-Sea Res., *21,* 911–931.

Green, J. S. A. 1970. Transfer properties of the large-scale eddies and the general circulation of the atmosphere. Quart. J. Roy. Meteor. Soc., *96,* 157–185.

Hogg, N. G. 1976. On spatially growing baroclinic waves in the ocean. J. Fluid Mech., *78,* 217–235.

Holland, W. R., and L. B. Lin. 1975. On the generation of mesoscale eddies and their contribution to the oceanic general circulation. I. A preliminary numerical experiment. J. Phys. Oceanogr., *5,* 642–657.

Koshlyakov, M. N., and Y. M. Grachev. 1973. Meso-scale currents at a hydrophysical polygon in the tropical Atlantic. Deep-Sea Res., *20,* 507–526.

Lorenz, E. N. 1967. The Nature and Theory of the General Circulation of the Atmosphere, World Meteorological Organization, Geneva, 161 pp.

Mooers, C. N. K., L. M. Bogert, R. L. Smith and J. G. Pattullo. 1968. A compilation of observations from moored current meters and thermographs (and of complementary oceanographic and atmospheric data). Oregon Continental Shelf, August-September 1966. Oregon State University. Reference 68-5, 98 pp.

Nowlin, W. D., Jr., T. Whitworth, III, and R. D. Pillsbury. 1977. Structure and transport of the Antarctic Circumpolar Current at Drake Passage from short-term measurements. J. Phys. Oceanogr., *7,* 788–802.

Pillsbury, R. D., T. Whitworth III, W. D. Nowlin, Jr., and F. Sciremammano, Jr. 1979. Currents and temperatures as observed in Drake Passage during 1975. J. Phys. Oceanogr., Submitted.

Rhines, P. B. 1977. The dynamics of unsteady currents, *in* The Sea, Vol. 6. Goldberg, McCave, O'Brien and Steele, eds. Wiley, New York, 1048 pp.

Richman, J. G. 1976. Kinematics and energetics of the mesoscale mid-ocean circulation: MODE. Ph.D. Thesis, Massachusetts Institute of Technology—Woods Hole Oceanographic Institution, 205 pp.

Robinson, A. R., and J. C. McWilliams. 1974. The baroclinic instability of the open ocean. J. Phys. Oceanogr., *4,* 281–294.

Schmitz, W. J., Jr. 1977. On the deep general circulation in the Western North Atlantic. J. Mar. Res., *35,* 21–28.

Smith, P. C. 1976. Baroclinic instability in the Denmark Strait overflow. J. Phys. Oceanogr., *6,* 355–371.

Stone, P. H. 1972. A simplified radiative-dynamical model for the static stability of rotating atmospheres. J. Atm. Sci., *29,* 405–418.

—— 1974. The meridional variation of the eddy heat fluxes by baroclinic waves and their parameterization. J. Atm. Sc., *31,* 444–456.

Swallow, J. C. 1971. The *Aries* current measurements in the western North Atlantic. Phil. Trans. Roy. Soc., London A., *270,* 451–460.

Thompson, R. O. R. Y. 1971. Structure of the Anatarctic Circumpolar Current. J. Geophys. Res., *76,* 8694.

Vonder Haar, T. H., and A. H. Oort. 1973. New estimate of annual poleward energy transport by Northern Hemisphere oceans. J. Phys. Oceanogr., *3,* 169–172.

Yao, T. 1978. Some effects of topography and vertical shear on low-frequency ocean fluctuations. Ph.D. Thesis, School of Oceanography, Oregon State University.

Received: *13 January, 1978;* revised: *19 September, 1978.*